

## EFFECT OF HALIDE ANIONS ON ANODIC BEHAVIOUR AND PASSIVATION OF COPPER IN ALKALINE MEDIA

Sayed S. ABD EL REHIM and Essam E. FOAD

*Chemistry Department,*

*Faculty of Science, Ain Shams University, Cairo, Egypt*

Received August 11, 1994

Accepted August 14, 1995

The effect of  $\text{Cl}^-$  and  $\text{Br}^-$  on the anodic behaviour and passivation of copper metal in NaOH solution has been investigated by a potentiodynamic technique complemented with XPS analysis. In halide free solutions, the anodic polarization curves involve three anodic peaks correlated to the electroformation of  $\text{Cu}_2\text{O}$ ,  $\text{CuO}$  and  $\text{Cu}(\text{OH})_2$  on the anode surface. The presence of these species in the passive layer has been confirmed by XPS examination. An addition of the halide anions enhances the peak currents of anodic peaks and tends to rupture the passive layer inducing the pitting corrosion. The critical pitting potentials decrease with rising halide concentration while the alkali concentration has an opposite effect. The accelerating effect of  $\text{Cl}^-$  to pitting corrosion is greater than that of  $\text{Br}^-$ . The pitting corrosion was explained by an instantaneous nucleation and growth of anion salt nuclei. Three cathodic peaks on cyclic voltammetric curve were assigned to the electroreduction of pitting corrosion products,  $\text{Cu}(\text{II})$  and  $\text{Cu}(\text{I})$  oxides, respectively.

**Key words:** Passivation; Copper; Halides.

The electrochemical behaviour of copper metal has been extensively investigated in alkaline solutions by different techniques<sup>1-7</sup>. The potentiodynamic oxidation of this metal is very complex process. In some cases, two anodic peaks were observed on voltammetric curves. The first peak is due to the electroformation of  $\text{Cu}_2\text{O}$  while the second peak is attributed to the electroformation of  $\text{Cu}(\text{II})$  (ref.<sup>8</sup>). The X-ray diffraction<sup>4</sup> and XPS analysis<sup>7</sup> proved that the passive layer depends on the conditions of its formation. An additional small peak preceding the formation of  $\text{Cu}_2\text{O}$  can be assigned either to the electroformation of  $[\text{Cu}(\text{OH})_2]^-$  or electrosorption of oxygen species<sup>6</sup>. Moreover, Shams El Din et. al.<sup>9</sup> observed an anodic peak in the potential region of oxygen evolution and attributed it to the formation of  $\text{Cu}(\text{III})$  oxide.

The effect of halide ions on the electrochemical behaviour of copper in alkaline media was studied in refs<sup>10-14</sup>. The halide ions were found to cause a local breakdown of the oxide layer giving rise to pitting corrosion. de Chialvo et al.<sup>12</sup> postulated that the pitting corrosion in presence of  $\text{Cl}^-$  ions involves the competition between the passive layer formation and the nucleation and growth of  $\text{CuCl}$  layer in equilibrium with  $\text{Cu}(\text{I})$  chloride complexes in solution. When the salt nuclei reach the metal surface, the pit

growth is found. Secondary breakdown of the salt layer results in copper dissolution to Cu(II) soluble species<sup>15</sup>.

The aim of this work is to investigate the effect of Cl<sup>-</sup> and Br<sup>-</sup> anions on the stability and properties of protective film on a copper surface in NaOH solution.

## EXPERIMENTAL

Special pure copper rods (Johnson and Mathey Chemical, Ltd.) axially embedded in araldite holders with exposed circular area of 0.5 cm<sup>2</sup> were used as working electrodes. Each electrode was polished with successively finer grades of emery paper, then degreased with ethyl alcohol and finally washed by stream of double distilled water. The counter electrode was made from 0.3 cm<sup>2</sup> platinum sheet. Potentials were measured against a saturated calomel electrode (SCE) as a reference electrode. In order to avoid the contamination, the reference electrode was connected to the working electrode via a bridge with the Luggin-Haber capillary tip and filled with solution under test.

Solutions of 0.01 and 0.10 mol l<sup>-1</sup> NaOH with various concentrations of NaCl and NaBr were prepared using double distilled water. All chemicals were of analytical grade quality. Electrolytes were de-aerated with N<sub>2</sub> previously purified<sup>16</sup>.

Voltammetric measurements were performed under potentiostatic control using a 3-electrode potentiostat (Wenking, Model POS 73). The potential-current density (*E-i*) curves were recorded using an X-Y recorder (Omnigraphic 2000). Measurements were carried out at a room temperature.

The XPS analysis of the electrode surface was carried out after the potential sweep from -2 000 mV to +1 000 mV at the scan rate of  $\nu = 10 \text{ mV s}^{-1}$ . The electrodes were removed from the electrolyte and rinsed with double distilled water prior to measurements. A Perkin-Elmer 550 ESCA spectrometer with X-ray radiation (1 253.6 eV) and a pass-energy to  $25 \pm 0.5 \text{ eV}$  was used.

## RESULTS AND DISCUSSION

Typical voltammetric curves for a copper electrode in 0.01 mol l<sup>-1</sup> NaOH with the increasing concentrations of Cl<sup>-</sup> and Br<sup>-</sup> are given in Figs 1 and 2. Figure 3 shows the effect of Cl<sup>-</sup> ions on the electrochemical behaviour of copper in 0.10 mol l<sup>-1</sup> NaOH. In all cases, the potential sweep started at -2 000 mV, with  $\nu = 10 \text{ mV s}^{-1}$ . It has been found that the shape of curves depends to the great extent on the alkali concentration and on the kind and the concentration of halide.

In halide-free solutions, the cathodic current density decreases gradually during the sweep to positive potentials and changes its sign at zero current (corrosion) potential  $E_{\text{corr}}$ . The anodic current exhibits three anodic peaks I, II, and III prior to oxygen evolution. Peak I reflects the electroformation of Cu<sub>2</sub>O (refs<sup>10,12,17</sup>). The formation and growth of this oxide eventually passivates the anode and results in a decrease of the dissolution current density. The appearance of peak II can be ascribed to the electroformation of CuO (refs<sup>10,12,17</sup>). The passive layer at peak II thus may be a composite formed by an inner layer of Cu<sub>2</sub>O and an outer layer of CuO. On the other hand, Ak-Kharafi et al.<sup>11</sup> attributed the appearance of anodic peak III most probably to the formation of Cu(OH)<sub>2</sub> on the oxide surface.

It is evident from the present data (curves 1 in Figs 1–3) that the peak current densities ( $i_p$ ) of anodic peaks I, II, and III increase and their peak potentials  $E_p$  shift to more negative values with increasing NaOH concentration. It is probable that the anodic dissolution of copper anode in alkali solutions is affected by the diffusion of  $\text{OH}^-$  through the oxide layer. Therefore, the increase of the peak current densities with rising

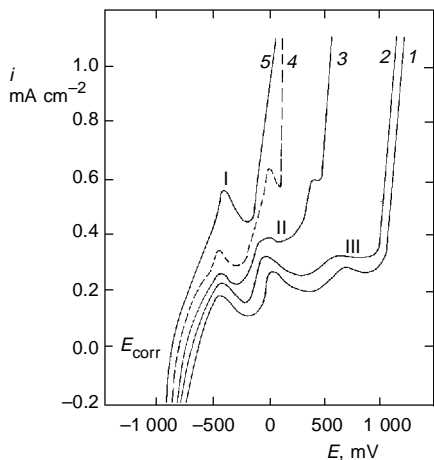


FIG. 1

Voltammograms for copper in  $0.01 \text{ mol l}^{-1}$  NaOH at various concentrations of NaCl: 1 0.0, 2 0.01, 3 0.1, 4 0.5, 5  $1.0 \text{ mol l}^{-1}$ ;  $\nu = 10 \text{ mV s}^{-1}$

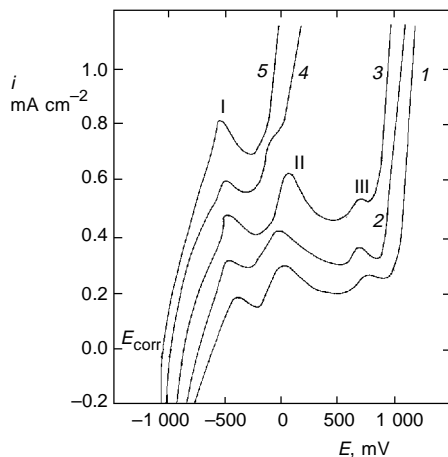


FIG. 2

Voltammograms for copper in  $0.01 \text{ mol l}^{-1}$  NaOH at various concentrations of NaBr: 1 0.0, 2 0.01, 3 0.1, 4 0.5, 5  $1.0 \text{ mol l}^{-1}$ ;  $\nu = 10 \text{ mV s}^{-1}$

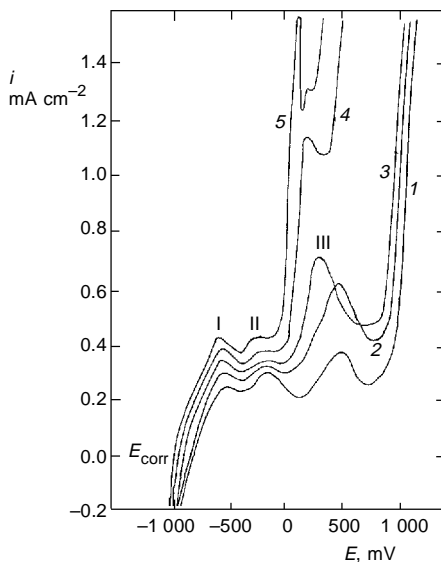


FIG. 3

Voltammograms for copper in  $0.1 \text{ mol l}^{-1}$  NaOH at various concentrations of NaCl: 1 0.0, 2 0.1, 3 0.5, 4 1.0, 5  $1.5 \text{ mol l}^{-1}$ ;  $\nu = 10 \text{ mV s}^{-1}$

alkali concentration can be ascribed part by to the increase of the rate of  $\text{OH}^-$  diffusion through the passive layer and part by to the increasing effect of  $\text{OH}^-$  on dissolution of anodically formed copper oxides.

The formation of soluble products has been reported by several authors. Miller<sup>8</sup> and Strehblow<sup>7</sup> observed the presence of Cu(I) ions at potentials of anodic peak I and  $\text{CuO}_2^{2-}$  at potentials of anodic peak II. The existence of polymeric species  $[\text{Cu}_n(\text{OH})_{2n-2}]^{2+}$  has been reported for the chemical dissolution of  $\text{Cu}(\text{OH})_2$  in concentrated alkali hydroxide<sup>18</sup>.

In order to get more informations about the film formed on copper surface in halide-free alkali solution, an XPS analysis was used after scanning the electrode from  $-2\ 000$

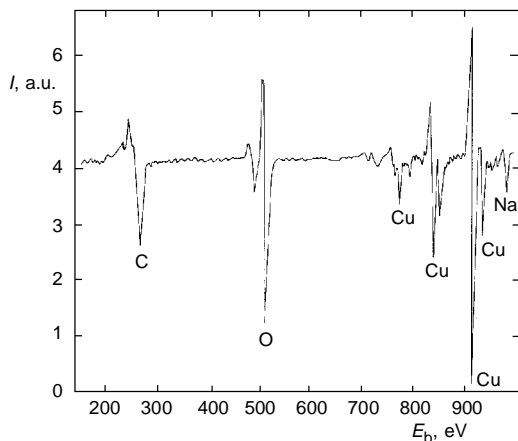


FIG. 4

XPS survey spectra (Auger) of the anodic film prepared potentiodynamically in  $0.01\ \text{mol l}^{-1}$  NaOH at the scan rate of  $10\ \text{mV s}^{-1}$ ,  $E_b$  binding energy

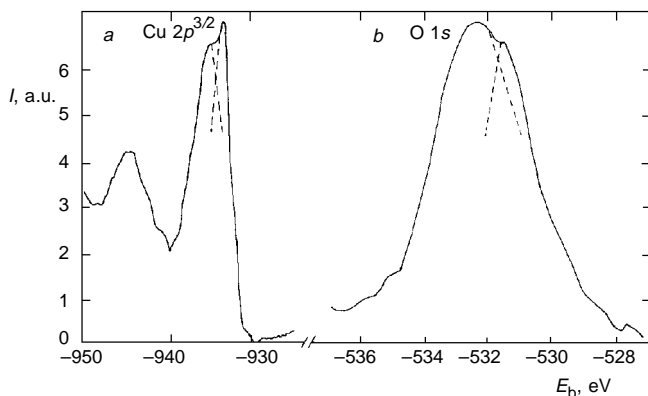


FIG. 5

XPS spectra of the anodic film prepared potentiodynamically in  $0.01\ \text{mol l}^{-1}$  NaOH at the scan rate of  $10\ \text{mV s}^{-1}$ . *a* Cu  $2p^{3/2}$  level, *b* O  $1s$  level;  $E_b$  binding energy

to +1 000 mV at  $v = 10 \text{ mV s}^{-1}$  in  $0.01 \text{ mol l}^{-1}$  NaOH solution. The XPS survey spectrum (Auger) of the passive film is shown in Fig. 4. The spectrum displays strong copper and oxygen peaks and weak peaks of Na and C; the latter may be attributed to the atmospheric contamination. The binding energies  $E_b$  of  $2p^{3/2}$  of copper and  $1s$  of oxygen bounds in the film are given in Figs 5a and 5b, respectively. The peak of O  $1s$  electron indicates various types of bound oxygen corresponding to binding energies of about 529.8, 531.8 and 533.0 eV, i.e.,  $\text{O}^{2-}$ ,  $\text{OH}^-$  and water physically adsorbed on the surface. However, the Cu  $2p^{3/2}$  spectrum exhibits two peaks at the binding energies of 932.2 and 933.5 eV and a small shake-up peak at 943.0 eV. According to the spectrum of oxygen and copper compounds<sup>19</sup>, the peak at 932.2 eV was assigned to  $\text{Cu}_2\text{O}$  while the peak at 933.5 eV can be attributed to  $\text{CuO}$  or  $\text{Cu}(\text{OH})_2$ . The spectrum of Cu  $2p^{3/2}$  signal does not allow to distinguish between  $\text{CuO}$  and  $\text{Cu}(\text{OH})_2$  at the surface. The appearance of the shake-up is also used for identification of  $\text{CuO}$  or  $\text{Cu}(\text{OH})_2$  (ref.<sup>10</sup>). Therefore, the XPS measurements support the view that the passive film is composed from  $\text{Cu}_2\text{O}$ ,  $\text{CuO}$  and  $\text{Cu}(\text{OH})_2$ .

From Figs 1–3, it follows that the addition of halide ion  $\text{X}^-$  ( $\text{X}^-$  represents  $\text{Cl}^-$  or  $\text{Br}^-$ ) to NaOH solution decreases the corrosion potential  $E_{\text{corr}}$ , enhances the peak current densities of the anodic peaks I–III and shifts their peak potentials to more negative values. The influence of  $\text{Br}^-$  on the increase of peak current is greater than that of  $\text{Cl}^-$ . The effect can be due to the adsorption of halides on the electrode surface and due to the formation of soluble  $\text{CuX}_2^-$  and  $\text{CuX}_3^-$  complexes<sup>8</sup>.

It is interesting that voltammetric curves exhibit a sudden rise of the anodic current density at a critical pitting potential  $E_{\text{pit}}$ , negative from the oxygen evolution. This behaviour indicates a pit initiation and propagation. An increase of the halide concentration shifts the pitting potential towards more negative (active) direction which corresponds to decreased resistance of protective layer to pitting. The dependence of  $E_{\text{pit}}$  on

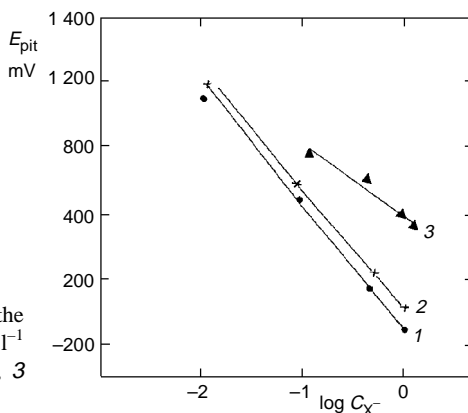


FIG. 6

Dependence of  $E_{\text{pit}}$  on  $\log C_{\text{X}^-}$  where  $C_{\text{X}^-}$  is the halide concentration in  $\text{mol l}^{-1}$ . 1  $0.01 \text{ mol l}^{-1}$  NaOH + NaCl, 2  $0.01 \text{ mol l}^{-1}$  NaOH + NaBr, 3  $0.1 \text{ mol l}^{-1}$  NaOH + NaCl

the concentration of  $X^-$  anions is given in Fig. 6. The  $E_{\text{pit}}$  vs  $\log C_{X^-}$  plots give straight lines according to the equation

$$E_{\text{pit}} = a - b \log C_{X^-} \quad (1)$$

where constants  $a$  and  $b$  depend on the alkali concentration and the type of the halide ion added. Inspection of this figure reveals that an increase of the alkali concentration increases the stability of the passive film towards pitting corrosion. Moreover, the accelerating effect of the halide ions toward pitting corrosion decreases in the order  $\text{Cl}^- > \text{Br}^-$ .

From the literature review for similar system<sup>12,15,17,20,21</sup> it can be concluded that the pitting corrosion of prepassivated copper in NaX solutions consists from sequence of stages involving the initial nucleation of CuX at weak points and defects of the passive oxide layer. This is followed by the salt nuclei penetration through the inner  $\text{Cu}_2\text{O}$  layer to the metal oxide interface where the dissolution of the base copper metal covered

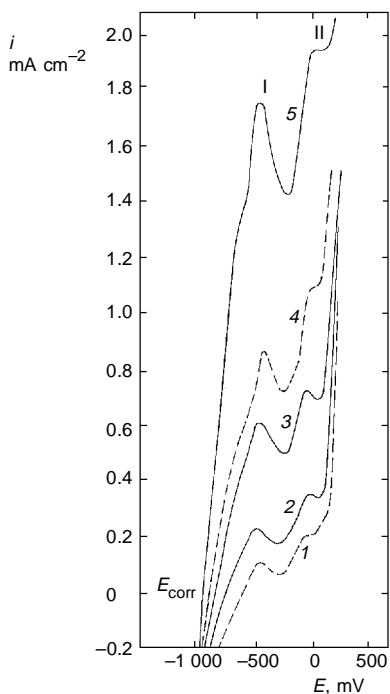


FIG. 7

Voltammetric curves for copper in  $0.01 \text{ mol l}^{-1}$  NaOH and  $0.1 \text{ mol l}^{-1}$  NaCl solution mixture at various sweep rates  $v$ : 1 5, 2 10, 3 20, 4 30, 5  $50 \text{ mV s}^{-1}$

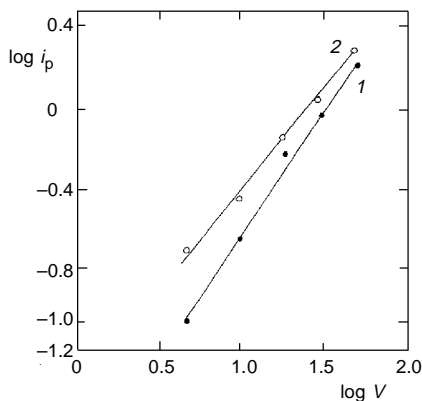


FIG. 8

The plot of  $\log i_p / \log v$  of the anodic peaks 1 I and 2 II. Data taken from Fig. 7

with  $\text{CuX}$  salt takes place. The corresponding reactions imply the local formation of different ionic species such as  $\text{CuX}_2^-$  and  $\text{CuX}_3^{2-}$  in equilibrium with  $\text{CuX}$ . The presence of soluble  $\text{Cu(II)}$  species can be explained as a secondary breakdown through the following reaction at the salt covered region involving  $\text{CuX}$  (ref.<sup>15</sup>).

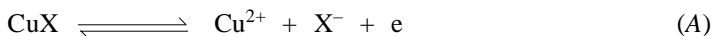


Figure 7 illustrates the influence of the scan rate on the voltammetric curves for copper anode in mixture of  $0.01 \text{ mol l}^{-1}$   $\text{NaOH}$  and  $0.1 \text{ mol l}^{-1}$   $\text{NaCl}$  solutions. Inspection of the curves reveals that an increase of the sweep rate causes a negative shift of the corrosion potential, but has no significant effect on the pitting potential  $E_{\text{pit}}$ . The plots of  $\log i_{\text{pI}}$  and  $\log i_{\text{pII}}$  against  $\log \nu$  are straight lines (Fig. 8). These data suggest that the oxidation process in the region of anodic peaks I and II is controlled by the diffusion of the reacting species. For that case, the following equation can be written<sup>22</sup>

$$\log i_{\text{p}} = a' + b' \log \nu, \quad (\text{2})$$

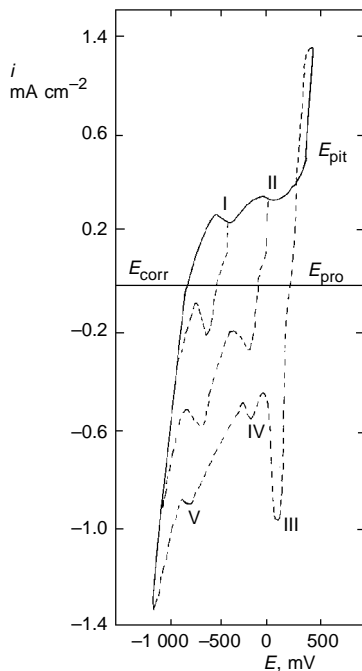


FIG. 9

Cyclic voltammograms of copper in  $0.01 \text{ mol l}^{-1}$   $\text{NaOH}$  and  $0.1 \text{ mol l}^{-1}$   $\text{NaCl}$  solution mixture at  $\nu = 10 \text{ mV s}^{-1}$  from  $-2000 \text{ mV}$  and reversed at various potentials

where  $a'$  and  $b'$  are constants,  $a'$  being function of concentration of the diffusion species, diffusion coefficient and the electrode area.

Figure 9 shows cyclic voltammograms for copper, electrode in 0.01 mol l<sup>-1</sup> NaOH and 0.01 mol l<sup>-1</sup> NaCl solution mixture from -2 000 mV, at  $\nu = 10$  mV s<sup>-1</sup> and the sweep reversed at various potentials. No cathodic peak appeared if the anodic sweep has been reversed at potentials more negative than that of peak I. Only one cathodic peak V has been observed if the anodic potential was reversed within the potential range of peak I. Two cathodic peaks IV and V appeared, however, if the anodic potential was reversed at potentials more positive than I and negative from  $E_{\text{pit}}$ . Peaks IV and V can be ascribed to the electroreduction of CuO and Cu<sub>2</sub>O oxides, respectively<sup>10</sup>. Finally, if the sweep was reversed at values more positive than  $E_{\text{pit}}$ , the scan exhibits hysteresis loop and pit propagation rate decreases rapidly reaching zero at the protective potential,  $E_{\text{pro}}$ , when all the pits repassivate<sup>23</sup>. Below  $E_{\text{pro}}$ , the reverse curve exhibits a new cathodic peak III, its appearance may be assigned to the electroreduction of pitting corrosion products<sup>24</sup>.

## REFERENCES

1. Ambrose J., Barradas R. G., Shoesmith D. W.: *J. Electroanal. Chem.* 47, 47 (1973).
2. Ambrose J., Barradas R. G., Shoesmith D. W.: *J. Electroanal. Chem.* 47, 65 (1973).
3. Shoesmith D. W., Lee W.: *Electrochim. Acta* 22, 1411 (1977).
4. Shoesmith D. W., Rummery T. E., Owen D., Lee W.: *J. Electrochem. Soc.* 124, 790 (1976).
5. Fletcher S., Barradas R. G., Porter J. D.: *J. Electrochem. Soc.* 125, 1960 (1978).
6. Droog J. M., Alderliesten C. A., Alderliesten P. T., Bootsma G. A.: *J. Electroanal. Chem.* 111, 61 (1980).
7. Strehblow H-H., Speckmann H. D.: *Werkst. Korros.* 35, 512 (1984).
8. Miller B.: *J. Electrochem. Soc.* 116, 1675 (1969).
9. Shams El Din M., Abd El Wahab F. M.: *Electrochim. Acta* 9, 113 (1964).
10. Strehblow H-H., Titzte B.: *Electrochim. Acta* 25, 839 (1980).
11. Al-Kharafi F. M., El-Tantawy Y. A.: *Corros. Sci.* 22, 1 (1982).
12. de Chialvo M. R. G., Salvarezza R. C., Vasquez Moll D. V., Arvia A. J.: *Electrochim. Acta* 30, 1501 (1985).
13. Drogowska M., Brossard L., Menard H.: *Corrosion-NACE* 43, 549 (1987).
14. de Chialvo M. R. G., de Mele M. F., Salvarezza R. C., Arvia A. J.: *Corros. Sci.* 28, 121 (1988).
15. Flatt R. K., Brook P. A.: *Corros. Sci.* 11, 185 (1971).
16. Gilroy D., Mayne J. E. O.: *J. Appl. Chem.* 12, 382 (1962).
17. Figueroa M. G., Salvarezza R. C., Arvia A. J.: *Electrochim. Acta* 31, 665 (1986).
18. Cotton A., Wilkinson G.: *Advanced Inorganic Chemistry*, 3rd ed. Wiley and Sons, Inc., London 1972.
19. Gaarenstroom W., Winograd N. W.: *J. Chem. Phys.* 67, 3500 (1977).
20. Galvele J. R.: *J. Electrochem. Soc.* 123, 464 (1976).
21. Okada T.: *J. Electrochem. Soc.* 131, 241 (1984).
22. Delahay P.: *New Instrumental Methods in Electrochemistry*, 1st ed. Interscience, New York 1954.
23. Wild B. E., Williams E.: *Electrochim. Acta* 16, 1971 (1971).
24. Abd El Rehim S. S., Taha F., Saleh M. B., Mohamed S. A.: *Corros. Sci.* 33, 1789 (1992).